



Contents lists available at ScienceDirect

Bioorganic & Medicinal Chemistry

journal homepage: www.elsevier.com/locate/bmc

Synthesis and evaluation of analogs of the phenylpyridazinone NPD-001 as potent trypanosomal TbrPDEB1 phosphodiesterase inhibitors and in vitro trypanocidals

Johan Veerman^a, Toine van den Bergh^a, Kristina M. Orrling^b, Chimed Jansen^b, Paul Cos^c, Louis Maes^c, Eric Chatelain^d, Jean-Robert Ioset^d, Ewald E. Edink^b, Hermann Tenor^e, Thomas Seebeck^f, Iwan de Esch^b, Rob Leurs^b, Geert Jan Sterk^{a,b,*}

^a Mercachem, PO Box 6747, 6503 GE Nijmegen, The Netherlands

^b Division of Medicinal Chemistry, Faculty of Sciences, Amsterdam Institute of Molecules, Medicines & Systems (AIMMS), Vrije Universiteit Amsterdam, De Boelelaan 1083, 1081 HV Amsterdam, The Netherlands

^c Laboratory for Microbiology, Parasitology and Hygiene (LMPH), University of Antwerp, Groenenborgerlaan 171, 2020 Wilrijk, Belgium

^d DNDi (Drugs for Neglected Diseases initiative), 15 Chemin Louis Dunant, 1202 Geneva, Switzerland

^e Takeda, Takeda Pharmaceuticals International GmbH, Thurgauerstrasse 130, 8152 Glattpark-Opfikon, Zurich, Switzerland

^f Institute of Cell Biology, University of Bern, Baltzerstrasse 4, 3012 Bern, Switzerland

ARTICLE INFO

Article history:

Received 18 December 2015

Revised 21 February 2016

Accepted 24 February 2016

Available online xxxx

Keywords:

Pyridazinone

Phosphodiesterase

Trypanosoma brucei

African trypanosomiasis

TbrPDEB1

Human PDEs

ABSTRACT

Trypanosomal phosphodiesterases B1 and B2 (TbrPDEB1 and TbrPDEB2) play an important role in the life cycle of *Trypanosoma brucei*, the causative parasite of human African trypanosomiasis (HAT), also known as African sleeping sickness. Knock down of both enzymes leads to cell cycle arrest and is lethal to the parasite. Recently, we reported the phenylpyridazinone, NPD-001, with low nanomolar IC₅₀ values on both TbrPDEB1 (IC₅₀: 4 nM) and TbrPDEB2 (IC₅₀: 3 nM) (*J. Infect. Dis.* **2012**, 206, 229). In this study, we now report on the first structure activity relationships of a series of phenylpyridazinone analogs as TbrPDEB1 inhibitors. A selection of compounds was also shown to be anti-parasitic. Importantly, a good correlation between TbrPDEB1 IC₅₀ and EC₅₀ against the whole parasite was observed. Preliminary analysis of the SAR of selected compounds on TbrPDEB1 and human PDEs shows large differences which shows the potential for obtaining parasite selective PDE inhibitors. The results of these studies support the pharmacological validation of the Trypanosome PDEB family as novel therapeutic approach for HAT and provide as well valuable information for the design of potent TbrPDEB1 inhibitors that could be used for the treatment of this disease.

© 2016 Elsevier Ltd. All rights reserved.

1. Introduction

Human African trypanosomiasis (HAT), or African sleeping sickness, is a neglected tropical disease that affects tens of thousands of patients annually.² The causative agent of this disease is the parasite *Trypanosoma brucei* (*T. brucei*), which is transmitted by the tsetse fly. The disease is fatal unless treated and current treatment options are limited.^{2–4} Consequently, the disease ranks high on the

list of Neglected Tropical Diseases for which there is an urgent need for more effective and less toxic medications.^{2–4}

Spatiotemporal control of the cyclic nucleotide signaling pathways is essential for any cell and disruption of this control may be detrimental to its survival.^{5,6} Cyclic nucleotide phosphodiesterases (PDEs) play a vital role in the control of the homeostasis of the intracellular cyclic nucleotides cAMP and cGMP in any eukaryotic cell. Inhibition of PDEs has therefore been recognized as an effective therapeutic concept in man (e.g., erectile dysfunction, chronic obstructive pulmonary disease (COPD) and psoriasis), and more recently also as a potential concept for the design of novel antiparasitic drugs.^{7–9}

The *T. brucei* phosphodiesterases TbrPDEB1 and TbrPDEB2 are essential for the survival of the bloodstream form of the parasite. Concomitant RNAi-induced knock-down of both enzymes kills

Abbreviations: MOE, Molecular Operating Environment; MW, microwave; TbrPDEB1, *Trypanosoma brucei* phosphodiesterase B1; TbrPDEB2, *Trypanosoma brucei* phosphodiesterase B2.

* Corresponding author.

E-mail address: g.j.sterk@vu.nl (G.J. Sterk).

the parasite in vitro and also saves mice from parasitaemia in vivo.⁵ Next to this genetic evidence, pharmacological validation of the TbrPDEB family as therapeutic target has been performed using the potent tetrazole-containing phenylpyridazinone **1** (NPD-001, previously reported as compd **A**)¹ and its pyrazolone analog, **2** (VUF13525)¹⁰ and a series of piclamilast (**3**) analogs with low micromolar activity against both TbrPDEB1 and -B2¹¹ (see Fig. 1).

Other chemical classes of PDE inhibitors have been investigated as well for TbrPDEB1 inhibition but only with minor results.^{12–17}

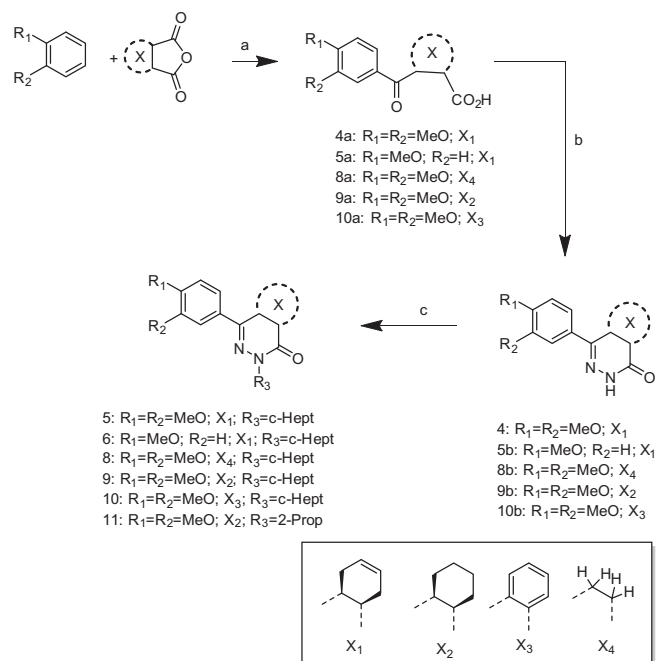
The phenylpyridazinone **1** shows low nanomolar inhibitory activities against both TbrPDEB enzymes (TbrPDEB1: IC₅₀ = 4 nM; TbrPDEB2: IC₅₀ = 3 nM), increases cAMP levels in the whole parasites and prevents cytokinesis, resulting in multinucleated, multi-flagellated cells that eventually lyse, resulting in potent in vitro trypanocidal activity against the bloodstream form of *Trypanosoma brucei*.¹ NPD-001 was originally described as a potent PDE4 inhibitor with sub-nanomolar potency,¹⁸ limiting its use as anti-trypanocidal.¹ This limitation does not stem from the side effects of PDE4 inhibitors per se but mainly from its TNF α suppressive effect as this cytokine plays a crucial role in host defense during infections.^{19–21} TNF α suppression makes a patient more vulnerable to infections which is a very undesirable condition in rural Africa.

However, as most potent TbrPDEB1 and -B2 inhibitor to date, NPD-001 is an interesting scaffold for hit exploration and SAR development. To evaluate the usefulness of the phenylpyridazinone scaffold for the design of a parasite-specific TbrPDEB1 inhibitor, we report here on a series of phenylpyridazinone analogs and their inhibitory activities on both TbrPDEB1 and on *Trypanosoma brucei* growth inhibitory activity in the Alamar blue test.

2. Results

2.1. Synthesis

The synthesis Schemes 1 and 2 depict the synthetic routes of all compounds, some of which (**1**, **4**, **5**, **9**, **11** and **14–18**) have been published before as PDE4 inhibitors,^{18,22} while the others (**6**, **7**, **8**, **10**, **12**, **13**, **19–25**) are new. For the compounds with the 3,4-dimethoxy (**4**, **5**, **8–11**) and the 4-methoxy (**6**) substitution the synthesis route (Scheme 1) started with a Friedel–Craft acylation. Subsequent condensation with hydrazine gave the pyridazinones which could be alkylated using sodium hydride in DMF. In all other cases (**1**, **7**, **12–25**) the route started with a Grignard reaction (Scheme 2) to obtain the gamma-ketopropionic acids. These carboxylic acids were then converted to the corresponding pyridazinones using the same chemistry as already outlined in Scheme 1. For the preparation of **1** and **12–25** the 3-cyclopentyloxy group of intermediate **1c** was hydrolyzed by 4-toluenesulfonic acid in toluene in a Dean Stark apparatus.¹⁸ The obtained phenol was then substituted to obtain the desired compounds using different conditions. The bromoalkyl intermediate **1e** was further derivatized by reacting with a phenol (**1f**, **14**, **17a**) or 5H-pyrrolo[3,2-d]pyrimidine (**15**). The nitrile **1f** was converted to the tetrazole **1** using sodium azide and ammonium chloride while the ester **17e** was hydrolyzed



Scheme 1. Synthetic route via Friedel–Craft acylation. Reagents: (a) AlCl₃ DCM, rt, 16 h. (b) EtOH, N₂H₄, reflux, 2 h. (c) DMF/NaH, R₃-Br, 0 °C, 20 min; rt, 16 h.

by potassium hydroxide to **17**. The methyl-substituted tetrazoles **12** and **13** were prepared as mixture by alkylation of **1** and purified by preparative HPLC. The regioisomer identity of the two methyl isomers was established using NMR experiments; NOESY, HSQC and HMBC.

All compounds, except the achiral **8** and **10**, were prepared as racemic mixtures of the *cis*-diastereomers (4aS,8aR and 4aR,8aS).

2.2. Pharmacological testing

All analogs were tested in at least two independent experiments for inhibition of TbrPDEB1-mediated [³H]-cAMP hydrolysis, using a scintillation proximity assay as described previously.¹ Selected compounds were tested for inhibition of *T. brucei* bloodstream form trypanostigote proliferation and for cytotoxicity on MRC-5 fibroblasts using established techniques.^{23,24} The antiparasitic effect of the compounds was determined for the subspecies *T. brucei brucei*, which is not infective to humans.

At this early stage of research, assessment of TbrPDEB2 inhibition was omitted, as suppression of parasite proliferation would imply concomitant inhibition of TbrPDEB1 and TbrPDEB2. In addition, two previous studies on TbrPDE inhibitors suggest high degree of equipotency against the paralogues,^{1,10} as expected from the high sequence homology. The binding sites of these two enzymes are completely identical and the sequence identity of the catalytic domain is 88%, of which the major discrepancies occur

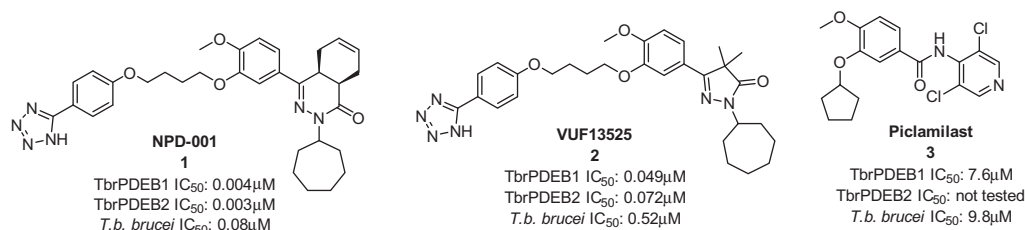
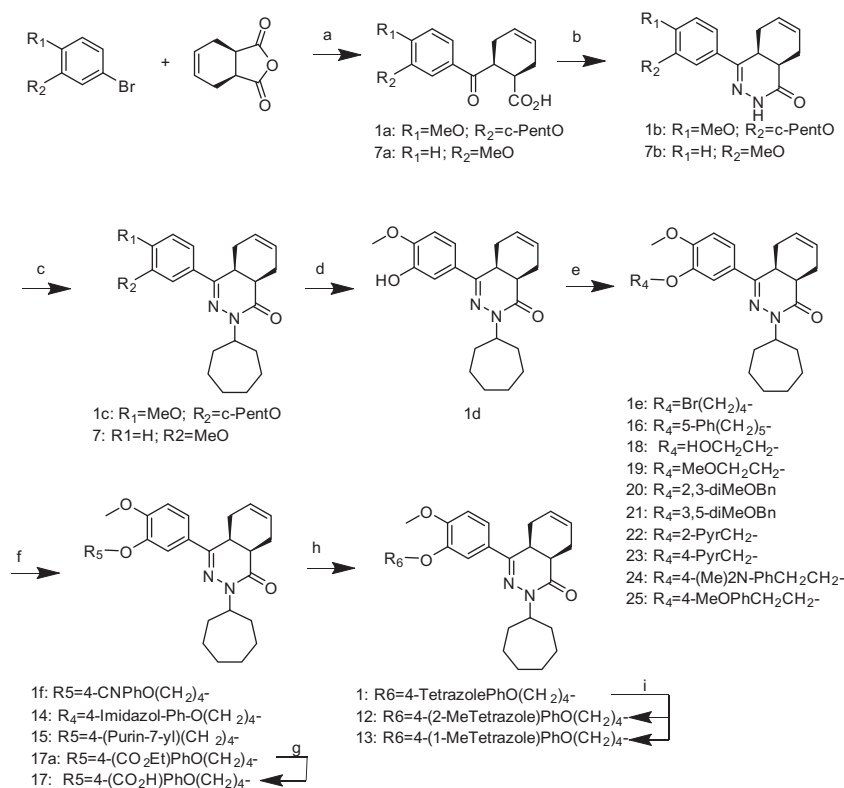


Figure 1. Known TbrPDE inhibitors with antitrypanosomal activity; **1**,¹ **2**,¹⁰ and **3**.¹¹



Scheme 2. Synthetic route via Grignard reaction. Reagents: (a) THF/Mg, 2 h, reflux, rt, anhydride, 18 h, 1 h reflux. (b) EtOH, N₂H₄, reflux, 2 h. (c) DMF/NaH, bromocycloheptane. (d) Toluene, 4-TsOH, 4 h Dean–Stark. (e) DMF/K₂CO₃, R–Br, 60 °C, 2 h or PPh₃–DIAD, THF, 0 °C. (f) DMF/K₂CO₃, ROH or R_xNH, 60 °C, 2 h. (g) KOH/H₂O/THF. (h) DMF/NaN₃/NH₄Cl, 8 h, 120 °C. (i) DMF/K₂CO₃, MeI, MW, 145 °C, 20 min.

in a single stretch of 33 amino acids in a mostly solvent-exposed loop.¹⁰

2.3. SAR analysis

For hit exploration of **1** a series of close analogs were prepared or collected from an earlier PDE4 inhibitor optimization project and screened against TbrPDEB1. **Table 1** shows analogs lacking the long tetrazole containing side chain. A direct comparison of **1** with **5** shows the impact of this tetrazole containing side chain: an 80-fold increase in inhibitory potency at TbrPDEB1. Also the cycloheptyl moiety is important for PDE inhibition, as demonstrated by a comparison of **4** and **5**. Removal of the cycloheptyl ring results in a 40 fold reduction in potency on TbrPDEB1. These results, with regards to the introduction of the cycloheptyl, are comparable to what was reported for a series of pyrazolones with TbrPDEB1 inhibiting activity.¹⁰

The results obtained with **5**, **6** and **7** indicate that the two methoxy groups are important for high inhibitory potency. Removal of the 3-methoxy substituent (**6**) results in a 13 fold reduction of potency while the 4-methoxy group is even more important, as removal (**7**) makes the compound approximately 300 fold less active. Comparison of **5** and **8** shows that the cyclohexene ring also has a strong influence on the activity (approximately 30 fold). The difference in potency between **5** and **9** is remarkable: the introduction of the double bond in the cyclohexyl ring gives a 5 fold increase in potency. Aromatization of the cyclohexyl ring (**10**) is clearly detrimental for inhibiting TbrPDEB1. Compounds **9** and **11** are equipotent showing that the cycloheptyl group at position R₃ can be replaced by an isopropyl without significant loss in activity. This finding might be important in future optimization programs when trying to reduce molecular size and lipophilicity,

Table 1
Inhibitory potency of selected phenylpyridazinones against TbrPDEB1

Compd	R ₁	R ₂	R ₃	Ring X	TbrPDEB1 ^a
4	MeO	MeO	H	X ₁	4.9
5	MeO	MeO	c-Heptyl	X ₁	6.5
6	MeO	H	c-Heptyl	X ₁	5.4
7	H	MeO	c-Heptyl	X ₁	4.0
8	MeO	MeO	c-Heptyl	X ₄	5.0
9	MeO	MeO	c-Heptyl	X ₂	5.8
10	MeO	MeO	c-Heptyl	X ₃	<5.0
11	MeO	MeO	2-Propyl	X ₂	5.7
1					8.4

^a –logIC₅₀ (n = 2, ±0.2).

though, evidently, it will be dependent on other substitutions on the scaffold as was observed with a series of pyrazolones were the effect of cycloheptyl/isopropyl replacements on TbrPDEB1 inhibiting potency varied between not significant to 31 fold.¹⁰

Methylation of **1** resulted in **12** and **13** of which the 2 substituted analog, **13**, is slightly less active though still very potent.

Changing the tetrazole ring of **1** to an imidazole ring (**14**) decreases TbrPDEB1 potency 3 fold while substituting it for a carboxylic acid (**17**) decreased potency approximately 80 fold. The purine analog **15** and the phenyl derivative **16** are both significantly less active than **1**. With the compounds **18–25** small variations in potencies on TbrPDEB1 is observed; a 2–5 fold increase in potency when compared with **5** (R=CH₃).

2.4. Growth inhibition

The compounds in Table 2 (except **17** and **22**) were also screened for anti trypanosomal activity in vitro and for cytotoxic activity on human fetal lung fibroblasts. In all cases, except **20**, there was at least a 10-fold difference between trypanocidal efficacy in the *T. brucei* growth inhibition assay and general cytotoxicity. The high efficacy of **1** in the anti trypanosomal assay, as compared to **12** and **13**, is remarkable. A potential explanation might be related to the tetrazole; Because of its pK_a of about 4.3 (calculated), **1** is present mostly in its anion form under physiological conditions, making it much less lipophilic and much better soluble under these conditions compared with its methylated analogs

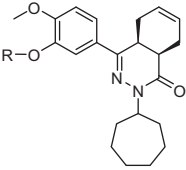
(solubility in 0.05 M phosphate buffer at pH = 7.4, containing 1% of DMSO, 75 μM for **1** vs <2 μM for **12** and **13**).

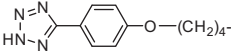
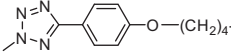
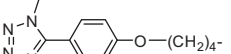
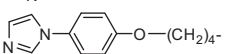

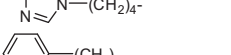
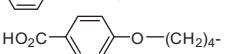
In Figure 2 a graphical presentation of the correlation between –logIC₅₀ on TbrPDEB1 and –logEC₅₀ on the whole parasite is given. In this correlation we left out the compounds with cLogP > 6 (**12**, **13**, **14**, **16**, **24**, **25**) except **1** (for of its good solubility at pH = 7.4) as being potential outliers because of their high lipophilicity and potential poor aqueous solubility. With this selection of compounds we calculated a fairly good correlation coefficient (R² = 0.92).

2.5. Cytotoxicity

For cytotoxicity assessment, selected compounds were tested against human cell line MRC-5. The selectivity index, SI, was expressed as the ratio between EC₅₀ in the parasite assay and CC₅₀ in the MRC-5 assay. An excellent selectivity index was found for 4 compounds, the tetrazole derivatives **1**, **12**, **13** and the purine **15**: >125–316. However the results with very lipophilic compounds might be obscured by their poor aqueous solubility (<2 μM for the methylated tetrazoles). Only 1 compound from this series, **20**, has a very poor selectivity index of 2.5, while the other analogs have a moderate SI between 12.6 and >63.

Table 2
Inhibitory activity against TbrPDEB1, *T. b. brucei* proliferation and cytotoxicity of close analogs of NPD-001



Compd	R	TbrPDEB1 ^a	<i>T. b. brucei</i> ^b	MRC-5 ^c	SI ^d	tPSA ^e	cLogP ^f
1		8.4	7.7	5.2	316	110	6.0
12		8.5	6.6	<4.2	>251	101	6.0
13		8.0	6.3	<4.2	>125	101	6.3
14		7.9	6.0	4.4	40	76	6.5
15		7.8	6.7	4.4	200	92	3.9
16		7.2	5.3	<4.2	>13	51	7.6
17	HO ₂ C– 	6.5	n.t. ^g	n.t. ^g		98	6.4
18	Hydroxyethyl	7.0	5.7	4.5	16	71	3.2
19	Methoxyethyl	7.1	6.1	4.6	32	60	3.9
20	2,3-Dimethoxybenzyl	7.1	5.8	5.4	2.5	71	5.5
21	3,5-Dimethoxybenzyl	6.9	6.0	4.9	12.6	71	5.8
22	2-Pyridylmethyl	7.0	n.t. ^g	n.t. ^g		64	4.3
23	4-Pyridylmethyl	6.8	5.9	4.8	12.6	64	4.3
24	4-N(CH ₃) ₂ -phenylethyl	7.2	6.0	<4.2	>63	54	6.3
25	4-MeO-phenylethyl	7.2	5.9	<4.2	>50	60	6.1

^a –logIC₅₀ on TbrPDEB1 (n = 2, ±0.2).

^b –logEC₅₀ on *T. b. brucei* (n = 2, ±0.2).

^c –logCC₅₀ on MRC-5 cells (n = 2, ±0.4).

^d Selectivity index: CC₅₀ MRC-5/EC₅₀ *T. b. brucei*.

^e Topological polar surface area.

^f Calculated logP.

^g Not tested.

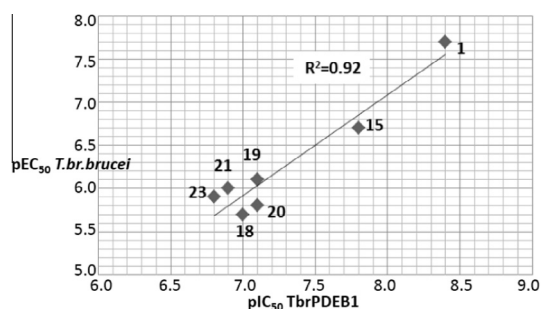


Figure 2. Correlation between $-\log IC_{50}$ TbrPDEB1 and $-\log EC_{50}$ *T. b. brucei*.

2.6. The parasite specific P-pocket

A special feature of TbrPDEB1 is the so-called parasite specific P-pocket. This pocket was first observed in the *Leishmania major* phosphodiesterase LmjPDEB1²⁵ and is shown to exist in TbrPDEB1 as well,²⁶ while it is absent in the human PDEs.²⁵ Targeting this pocket might lead to parasite specific PDE inhibitors.²⁵

The high TbrPDEB1 inhibiting potency of **1** as compared with **5** can be hypothesized to originate from interaction of the tetrazole containing side chain with this pocket. In silico docking experiments, using the X-ray apo structure of TbrPDEB1,²⁶ confirmed this possibility (Fig. 3). In this docking experiment the phenylpyridazinone scaffold was positioned in the hydrophobic clamp, which consists of phenylalanine (F877) and valine (V840), while the two ether functions were positioned to interact with the invariant glutamate (Q874). The tetrazole moiety moved in the direction of the P-pocket, interacting with a tyrosine (Y845). No further docking studies, with different ligands, were undertaken because of multiple possible binding modes with these flexible side chains. The next step in this research would be using X-ray crystallography to study the interaction of PDE inhibitors with the enzyme to assess the value of the P-pocket in designing parasite selective PDE inhibitors.

2.7. PDE selectivity panel

As most potent TbrPDEB inhibitor, we tested NPD-001 **1** on a panel of human PDEs to verify subtype potency and the results are summarized in Table 3 and visualized in Figure 4. Besides being a potent low nanomolar inhibitor of TbrPDEB1 and TbrPDEB2, the compound shows the previously reported sub-nanomolar potencies at the human PDE4 isoenzymes and only interacts with the

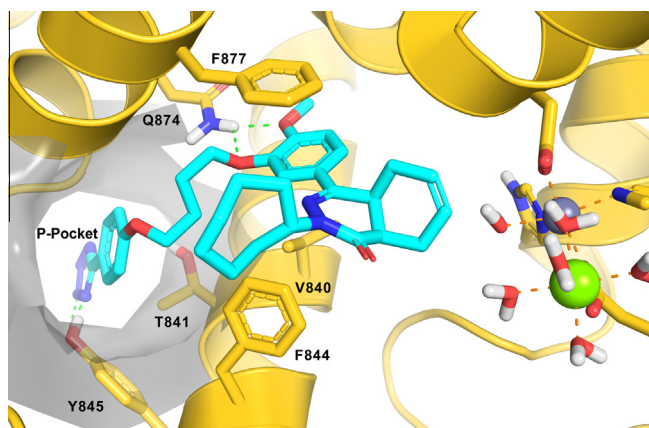


Figure 3. Proposed binding mode of NPD-001 (blue sticks) in TbrPDEB1. The P-pocket is indicated by the gray molecular surface.

Table 3

Inhibitory potency of **1** against a panel of human PDEs and TbrPDEB1 and TbrPDEB2

Enzyme	pIC ₅₀ ^a	Enzyme	pIC ₅₀
TbrPDEB1	8.4	hPDE4D3	9.2
TbrPDEB2	8.5	hPDE5A1	5.7
hPDE1B1	5.4	hPDE7A1	5.5
hPDE2A3	5.2	hPDE8B	5.4
hPDE3A1	6.9	hPDE9A3	<5.0
hPDE4B1	9.2	hPDE10A	6.3
hPDE4B2	9.3	hPDE11A4	5.7

^a $-\log IC_{50}$ ($n = 2, \pm 0.2$).

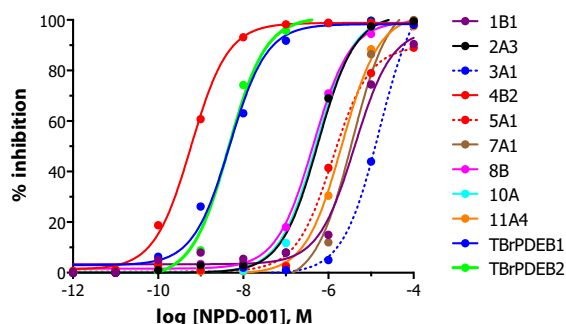


Figure 4. Dose response curves of **1** against a panel of human PDEs, TbrPDEB1 and TbrPDEB2.

other human PDEs in high nanomolar and micromolar concentrations, suggesting that for this series of molecules human PDE4 is the main off-target.

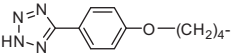
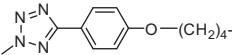
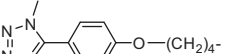
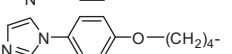

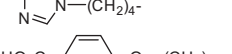
2.8. Inhibition of TbrPDEB1 versus human PDE4

From the above described human PDE panel screen of **1** it is clear that especially PDE4 inhibition will limit the usefulness of this compound. In order to find clues for optimization towards TbrPDEB1 selectivity over all human PDEs we tested a selection of phenylpyridazinones against the human PDE4 subtype (Table 4). With these 7 compounds in Table 4, a 100 fold variation in TbrPDEB1 inhibiting potency was observed while with the same compounds the variation on hPDE4B1 inhibition was only 8 fold. Direct comparison of **1** and **5** shows the effect of the tetrazole containing side chain: these 2 compounds are equipotent on PDE4 while there is an 80 fold difference on the parasite PDE. From these data we calculated for each individual compound the ratio between IC_{50} on the parasite and this human PDE, showing variation from 6 to 1000. These variations are clearly indicative for significant differences in SAR between TbrPDEB1 and human PDE4B1, making it likely that optimization for TbrPDEB1 selectivity over human PDE4 is possible.

3. Conclusions

For reasons of hit validation of **1** we collected a series of NPD-001 analogs by synthesis and from the shelves from a project for human PDE4 inhibitors and determined their TbrPDEB1 inhibiting activities. For some analogs the in vitro antiproliferative activity on *Trypanosome brucei* was determined as well. Analysis of the structure activity relationships shows that within this series of pyridazinones the TbrPDEB1 inhibiting potency varies 25,000 fold (compare **1** with **7**). Comparison of the 3,4-dimethoxy compound **5** with **1** shows an 80 fold difference in potency, which is speculated to originate from interaction of the tetrazole with the parasite specific P-pocket and is supported by molecular docking studies.

Table 4
Inhibitory potency of some analogs of **1** against TbrPDEB1 and hPDEB1

Compd	R	TbrPDEB1 ^a	hPDE4B1 ^b	IC ₅₀ TbrPDEB1/IC ₅₀ hPDE4B1
5	CH ₃	6.5	9.2	501
1		8.4	9.2	6
12		8.5	9.3	6
13		8.0	9.2	16
14		7.9	9.7	63
15		7.8	8.8	10
17		6.5	9.5	1000

^a –log IC₅₀ on TbrPDEB1 (*n* = 2, ±0.2).^b –log IC₅₀ on human PDE4B1 (*n* = 2, ±0.2).

Comparison of TbrPDEB1 IC₅₀ with antiproliferative EC₅₀ showed good correlation between biochemical activity on the parasite PDE and in vitro antiproliferative activity on the whole parasite; this result gives further target validation of the *Trypanosome* PDEs.

The most potent compound in this study (**1**) is however a significantly more potent inhibitor of the human PDE4 subtypes than of TbrPDEB1. To have any potential in the treatment of human African trypanosomiasis significant selectivity for the parasite PDE over the human PDEs is essential. This is especially important for hPDE4 as inhibition of this subtype will compromise a patient's immune system. These compounds clearly do not fulfill this requirement yet, as shown by **1**, which is 6–9 times more potent on the hPDE4 subtypes. Still, preliminary analysis of the activities of selected compounds on both TbrPDEB1 and human PDE4B1 shows significant SAR differences which is indicative for the potential of obtaining TbrPDEB1 selectivity over human PDE4.

We believe that the potencies of these compounds on TbrPDEB1, their SAR on both the parasite PDE and human PDEs, as well as their potency in inhibiting trypanosomal growth in vitro and their weak cytotoxicity warrants further investigations of this chemical class towards a novel PDE inhibition based treatment of this disease.

4. Experimental section

4.1. Molecular docking

The 4aS,8aR enantiomer of **1** was built manually using MOE²⁷ (version 2012.10). After energy minimization (MMF94x) the molecule was stored in a MOE database file and the tetrazole moiety was deprotonated using the MOE Wash function. A mol2 file was generated and used as input for PLANTS.²⁸ The A chain of the apo TbrPDEB1 crystal structure (pdb: 4I15) was prepared for docking using MOE (version 2012.10) by adding and minimizing the hydrogen atoms using the protonate 3D function. The water molecules and metal ions were removed from the structure. The pocket of the protein was manually defined (Y668, H669, N717, T783, M785, N822, I823, N825, V826, S833, W836, A837, V840, T841, F844, Y845, L859, M861, F862, N867, M868, E869, L870, G873, Q874, F877) and both the protein and the pocket were stored in mol2 format as input for PLANTS. The 4aS,8aR enantiomer of **1** was docked 25 times using the speed 1 setting of PLANTS and

the chemPLP scoring function. The generated docking poses were visually inspected for formation of hydrogen bonds between the oxygen atom of the methoxy group of compound **1** and the nitrogen atom of the carboxamide moiety of Q874. Interestingly, for both tetrazole tautomers (1*H* or 2*H*) the highest ranked pose that displayed this anticipated interaction was in both cases pose 7 of the 25 generated poses. Both binding poses were very similar and in both cases the parasite-selective P-pocket was being addressed by the tetrazolephenoxy moiety.

4.2. Synthetic chemistry

4.2.1. General information

All compounds have been analyzed by ¹H NMR (Bruker, 400 MHz or 500 MHz) and analytical LCMS for identity and purity. (Apparatus: Agilent 1100 Bin. Pump: G1312A, degasser; autosampler, ColCom, DAD: Agilent G1315B, 220–320 nm, MSD: Agilent LC/MSD G1946D ESI, pos/neg 100–800, column: Waters XBridge™ C18, 50 × 2.1 mm, 3.5 μ, Temp: 35 °C, Flow: 0.8 mL/min, Gradient: *t*₀ = 2% A, *t*_{3.5min} = 98% A, *t*_{6min} = 98% A, Posttime: 2 min; Eluent A: 0.1% formic acid in acetonitrile, Eluent B: 0.1% formic acid in water). Exact molecular masses (HRMS) were determined on a Bruker microTOF-Q mass spectrometer equipped with an electrospray ion source using caffeine as reference. The purity of all compounds was >95%. The synthesis of the compounds **1**, **4**, **5**, **9**, **11** and **14–18** has been described before.^{18,22,29,30} and the remaining compounds (**6**, **7**, **8**, **10**, **12**, **13**, **19–25**) are prepared in an analogous manner and shortly described below.

Method A: Methoxybenzene or 1,2-dimethoxybenzene (50 mmol) was added to a suspension of aluminiumtrichloride (6.67 g, 50 mmol) in DCM (100 ml) at 0 °C. After complete addition, *cis*-1,2,3,6-tetrahydrophthalic anhydride or phthalic anhydride (50 mmol) was added. After 5 h at rt, the mixture was poured onto ice. The organic layer was dried over MgSO₄ and evaporated. The residue was triturated with diethyl ether and dried; yield 40–60%.

Method B: A solution of 3-methoxybromobenzene (3.74 g, 20 mmol) in dry THF was added slowly to a suspension of Mg(s) (0.53 g, 22 mmol) in THF and the resulting mixture refluxed for 5 h, after which it was added slowly to a solution of *cis*-1,2,3,6-tetrahydrophthalic anhydride (3.04 g, 20 mmol) in THF. The mixture was stirred at room temperature for 18 h and subsequently quenched with ammonium chloride. Next the mixture was acidified with hydrochloric acid (2 N) and the mixture extracted with

diethyl ether. The ether solution was dried over MgSO_4 and evaporated. The residue was triturated with diethyl ether; yield 40–50%.

Method C: A solution of a ketocarboxylic acid (10 mmol) and hydrazine- H_2O (0.60 g, 12 mmol) in ethanol (150 ml) was refluxed for 6 h. After cooling to room temperature the precipitate was filtered off and dried; yield 80–90%.

Method D: NaH (0.22 g, 5.5 mmol, 60% mineral oil) was added to a suspension of a pyridazinone (5 mmol) in DMF and the resulting mixture was stirred for 30 min. After addition of bromocycloheptane (1.06 g, 6 mmol) the mixture was stirred at room temperature for 18 h and subsequently poured into water. The resulting mixture was extracted with diethyl ether, the ether layer was dried over MgSO_4 and evaporated. The residue was purified by column chromatography (ethyl acetate hexane gradients); yield 50–80%.

Method E: A mixture of 55 mmol of 4-toluenesulfonic acid-hydrate (10.46 g, 55 mmol) and *cis*-2-cycloheptyl-4-(3-cyclopentyloxy-4-methoxy-phenyl)-4a,5,8,8a-tetrahydro-2H-phthalazin-1-one (**19a**) (21.83 g, 50 mmol) in toluene (250 ml) was refluxed in a Dean–Stark as described previously.¹²

Method F: A mixture of *cis*-2-cycloheptyl-4-(3-hydroxy-4-methoxy-phenyl)-4a,5,8,8a-tetrahydro-2H-phthalazin-1-one¹² (0.70 g, 1.9 mmol), K_2CO_3 (0.53 g, 3.8 mmol) and alkylating agent (3.4 mmol) in DMF (20 ml) was stirred at 65 °C upon completion (2–6 h). Then the reaction was quenched with water and the resulting mixture was extracted with ethyl acetate. The organic layers were combined and washed with sodium bicarbonate (aq, satd) and water and subsequently dried over Na_2SO_4 and evaporated. The residue was purified by flash chromatography (ethyl acetate hexane gradients).

Method G: A solution of diisopropyl azodicarboxylate (67 mg, 0.33 mmol) in THF (2 ml) was added dropwise to an ice-cooled solution of *cis*-2-cycloheptyl-4-(3-hydroxy-4-methoxy-phenyl)-4a,5,8,8a-tetrahydro-2H-phthalazin-1-one,¹² (100 mg, 0.27 mmol), an alcohol (0.27 mmol) and 0.35 mmol triphenylphosphine (92 mg, 0.35 mmol) in THF (25 ml). After complete addition the reaction mixture was allowed to reach room temperature and the resulting mixture was stirred for 2 h. Next the reaction mixture was concentrated under reduced pressure, the residue partitioned between ethyl acetate and NaOH (aq, 1 M). The organic phase was washed with brine and subsequently dried over Na_2SO_4 and evaporated. The residue was purified by flash chromatography (ethyl acetate hexane gradients); yield 24%.

4.2.2. Synthetic details and spectroscopic data

4.2.2.1. *cis*-2-(4-Methoxybenzoyl)-1,2,3,6-tetrahydrobenzoic acid (5a). Method A, from 4-methoxybenzene (5.4 g, 50 mmol) and *cis*-1,2,3,6-tetrahydrophthalic anhydride (7.6 g, 50 mmol), followed by column chromatography using hexane/ethyl acetate + 1% AcOH = 19/1 to 1/1; Yield: 59%. LC–MS–ESI⁺ *m/z* 261 [M+H]⁺.

4.2.2.2. *cis*-4-(4-Methoxy-phenyl)-4a,5,8,8a-tetrahydro-2H-phthalazin-1-one (5b). Method C, from *cis*-2-(4-methoxybenzoyl)-1,2,3,6-tetrahydrobenzoic acid (**5a**, 2.6 g, 10 mmol) and hydrazine hydrate (0.60 g, 12 mmol). Yield: 74%; LC–MS–ESI⁺ *m/z* 257 [M+H]⁺.

4.2.2.3. *cis*-2-Cycloheptyl-4-(4-methoxy-phenyl)-4a,5,8,8a-tetrahydro-2H-phthalazin-1-one (6). Method D, from compound *cis*-4-(4-methoxy-phenyl)-4a,5,8,8a-tetrahydro-2H-phthalazin-1-one (**5b**, 1.28 g, 5 mmol) and bromocycloheptane (1.06 g, 6 mmol); Yield: 52%. ¹H NMR (CDCl_3): δ 7.76 (d, *J* = 9.0 Hz, 2H), 6.94 (d, *J* = 9.0 Hz, 2H), 5.74–5.82 (m, 1H), 5.62–5.71 (m, 1H), 4.76–4.86 (m, 1H), 3.85 (s, 3H), 3.25–3.32 (m, 1H), 2.95–3.06 (m, 1H), 2.72 (t, *J* = 6.0 Hz, 1H), 1.70–2.25 (m, 9H),

1.45–1.69 (m, 6H). LC–MS–ESI⁺ *m/z* 353 [M+H]⁺; HRMS–ESI⁺ [M+H]⁺ calcd for $\text{C}_{22}\text{H}_{29}\text{N}_2\text{O}_2$ 353.2224, found 353.2217.

4.2.2.4. *cis*-2-(3-Methoxybenzoyl)-1,2,3,6-tetrahydrobenzoic acid (7a). Method B, from 3-methoxybromobenzene and *cis*-1,2,3,6-tetrahydrophthalic anhydride, followed by column chromatography using hexane/ethyl acetate + 1% AcOH = 19/1 to 1/1; Yield: 41%. LC–MS–ESI⁺ *m/z* 261 [M+H]⁺; purity 82%.

4.2.2.5. *cis*-4-(3-Methoxy-phenyl)-4a,5,8,8a-tetrahydro-2H-phthalazin-1-one (7b). Method C, from *cis*-2-(3-methoxybenzoyl)-1,2,3,6-tetrahydrobenzoic acid (**7a**, 2.6 g, 10 mmol) and hydrazine hydrate (0.60 g, 12 mmol); Yield: 67%. LC–MS–ESI⁺ *m/z* 257 [M+H]⁺.

4.2.2.6. *cis*-2-Cycloheptyl-4-(3-methoxy-phenyl)-4a,5,8,8a-tetrahydro-2H-phthalazin-1-one (7). Method D, from *cis*-4-(3-methoxy-phenyl)-4a,5,8,8a-tetrahydro-2H-phthalazin-1-one (**7b**, 1.28 g, 5 mmol) and bromocycloheptane (1.06 g, 6 mmol); Yield: 53%. ¹H NMR (CDCl_3) δ 8.22 (dd, *J*1 = 2.0 Hz, *J*2 = 8.8 Hz, 1.0H), 8.04 (dd, *J*1 = 2.0 Hz, *J*2 = 8.8 Hz, 1.0H), 7.70 (m, 2H), 7.20 (m, 2H), 7.10 (m, 1H), 3.87, s, 6H), 3.61 (quintet, *J* = 7.0 Hz, 1H), 1.55 (m, 12H). LC–MS–ESI⁺ *m/z* 353 [M+H]⁺; HRMS–ESI⁺ [M+H]⁺ calcd for $\text{C}_{22}\text{H}_{29}\text{N}_2\text{O}_2$ 353.2224, found 353.2225.

4.2.2.7. 2-Cycloheptyl-6-(3,4-dimethoxy-phenyl)-4,5-dihydro-2H-pyridazin-3-one (8). Method D, from 6-(3,4-dimethoxyphenyl)-4,5-dihydro-2H-pyridazin-3-one²⁰ (1.17 g, 5 mmol) and bromocycloheptane (1.06 g, 6 mmol); crystallized from methanol. Yield: 64%. ¹H NMR (CDCl_3) δ 7.47 (d, *J* = 2.0 Hz, 1H), 7.22 (dd, *J* = 2.0, 8.4 Hz, 1H), 6.87 (d, *J* = 8.4 Hz, 1H), 4.78–4.86 (m, 1H), 3.94 (s, 3H), 3.92 (s, 3H), 2.87 (t, *J* = 7.8 Hz, 2H), 2.55 (t, *J* = 7.8 Hz, 2H), 1.78–1.92 (m, 6H), 1.50–1.65 (m, 6H). LC–MS–ESI⁺ *m/z* 331 [M+H]⁺; HRMS–ESI⁺ [M+H]⁺ calcd for $\text{C}_{19}\text{H}_{27}\text{N}_2\text{O}_3$ 331.2016, found 331.2013.

4.2.2.8. 2-Cycloheptyl-4-(3,4-dimethoxyphenyl)-2H-phthalazin-1-one (10). Prepared from 4-(3,4-dimethoxyphenyl)-2-phenyl-2H-phthalazin-1-one²⁰ (1.41 g, 5 mmol) and bromocycloheptane (1.06 g, 6 mmol) by method D. Crystallized from methanol; Yield: 71%. ¹H NMR (CDCl_3): δ 8.57–8.54 (m, 1H), 7.85–7.74 (m, 3H), 7.23–7.16 (m, 2H), 7.04 (d, *J* = 8.2 Hz, 1H), 5.26 (heptet, *J* = 4.7 Hz, 1H), 3.99 (s, 3H), 3.96 (s, 3H), 2.14–2.02 (m, 4H), 1.90–1.81 (m, 2H), 1.75–1.58 (m, 6H). LC–MS–ESI⁺ *m/z* 379 [M+H]⁺; HRMS–ESI⁺ [M+H]⁺ calcd for $\text{C}_{23}\text{H}_{27}\text{N}_2\text{O}_3$ 379.2016, found 379.2005.

4.2.2.9. *cis*-2-Cycloheptyl-4-(4-methoxy-3-(4-(4-(2-methyl-2H-tetrazol-5yl)phenoxy)butoxy)phenyl)-4a,5,8,8a-tetrahydrophthalazin-1(2H)-one (12) and *cis*-2-cycloheptyl-4-(4-methoxy-3-(4-(4-(1-methyl-1H-tetrazol-5-yl)phenoxy)butoxy)phenyl)-4a,5,8,8a-tetrahydrophthalazin-1(2H)-one (13). K_2CO_3 (242 mg, 1.752 mmol) and 2 ml of DMF was added to a 5 mL MW-vial with **1** (100 mg, 0.171 mmol) and MW irradiated at 145 °C for 20 min. Iodomethane (12 μL , 0.193 mmol) was added through the septum and the reaction mixture was MW irradiated at 145 °C for 30 min and then stirred at rt for 18 h. The reaction mixture was diluted with ethyl acetate 15 mL and washed with brine (3 \times 8 mL) in order to remove the DMF. The organic layer was dried over Na_2SO_4 , filtered and evaporated. The crude product was purified with flash column chromatography (Biotage Silicycle 25 g, silica, ethyl acetate in cyclohexane (10–70%, 2–10–3 CV) to give **12** (75.9 mg, 0.127 mmol, 72% yield) as the major component in the first eluted peak and **13** (19 mg, 0.032 mmol, 18% yield) as the minor component in the second eluted peak, resulting in a total yield of

95 mg (90%) with a regioisomer ratio of 4:1 major/minor. The position of the introduced methyl group was determined with 2D NMR experiments. **12**: ^1H NMR (500 MHz, CDCl_3) δ (ppm) 8.03 (appar. d, $J = 8.74$ Hz, 2H), 7.51 (appar. s, 1H), 7.27 (appar. d, $J = 8.76$ Hz, 1H), 6.98 (appar. d, $J = 8.87$ Hz, 2H), 6.87 (appar. d, $J = 8.45$ Hz, 1H), 5.77 (d, $J = 8.60$ Hz, 1H), 5.66 (d, $J = 8.40$ Hz, 1H), 4.87–4.78 (m, 1H), 4.36 (s, 3H), 4.21–4.15 (m, 2H), 4.15–4.08 (m, 2H), 3.88 (s, 3H), 3.27 (dt, $J = 11.45$, 5.74 Hz, 1H), 2.99 (br d, $J = 17.74$ Hz, 1H), 2.71 (t, $J = 5.68$ Hz, 1H), 2.23–1.95 (m, 8H), 1.95–1.85 (m, 1H), 1.84–1.69 (m, 4H), 1.65–1.46 (m, 6H); LC–MS–ESI $^+$ m/z 599 [M+H] $^+$; HRMS–ESI $^+$ [M+Na] $^+$ calcd for $\text{C}_{34}\text{H}_{42}\text{N}_6\text{O}_4\text{Na}$ 621.3160, found 621.3162. **13**: ^1H NMR (500 MHz, CDCl_3) δ (ppm) 7.69 (d, $J = 8.67$ Hz, 2H), 7.53 (s, 1H), 7.29 (d, $J = 10.23$ Hz, 1H), 7.07 (d, $J = 8.67$ Hz, 2H), 6.89 (d, $J = 8.44$ Hz, 1H), 5.78 (d, $J = 9.82$ Hz, 1H), 5.67 (d, $J = 10.08$ Hz, 1H), 4.91–4.78 (m, 1H), 4.22–4.13 (m, 4H), 4.16 (s, 3H), 3.90 (s, 3H), 3.29 (dt, $J = 11.48$, 5.72 Hz, 1H), 3.00 (d, $J = 18.31$ Hz, 1H), 2.72 (t, $J = 5.81$ Hz, 1H), 2.25–1.96 (m, 8H), 1.96–1.86 (m, 1H), 1.84–1.71 (m, 4H), 1.70–1.46 (m, 6H); LC–MS–ESI $^+$ m/z 599 [M+H] $^+$; HRMS–ESI $^+$ [M+Na] $^+$ calcd for $\text{C}_{34}\text{H}_{42}\text{N}_6\text{O}_4\text{Na}$ 621.3160, found 621.3173.

4.2.2.10. *cis*-2-Cycloheptyl-4-[4-methoxy-3-(2-methoxyethoxy)-phenyl]-4a,5,8,8a-tetrahydro-2H-phthalazin-1-one (19).

Method F, from 1-bromo-2-methoxyethane (473 mg, 3.4 mmol); In this case the reaction mixture was stirred for 4 h at 65 °C and the reaction mixture was quenched with hydrogen chloride (aq, 1 N) instead of water; Yield: 24%. ^1H NMR (CDCl_3) δ 7.54 (d, $J = 2.0$ Hz, 1H), 7.31 (dd, $J = 8.5$, 2.0 Hz, 1H), 6.88 (d, $J = 8.5$, 1H), 5.74–5.83 (m, 1H), 5.63–5.72 (m, 1H), 4.78–4.88 (m, 1H), 4.24 (t, $J = 5.0$ Hz, 2H), 3.90 (s, 3H), 3.81 (t, $J = 5.0$ Hz, 2H), 3.47 (s, 3H), 3.23–3.33 (m, 1H), 2.95–3.06 (m, 1H), 2.72 (t, $J = 5.5$ Hz, 1H), 1.86–2.26 (m, 5H), 1.45–1.86 (m, 10H). LC–MS–ESI $^+$ m/z 427 [M+H] $^+$; HRMS–ESI $^+$ [M+H] $^+$ calcd for $\text{C}_{25}\text{H}_{35}\text{N}_2\text{O}_4$ 427.2591, found 427.2578.

4.2.2.11. *cis*-2-Cycloheptyl-4-[3-(2,3-dimethoxybenzyloxy)-4-methoxy-phenyl]-4a,5,8,8a-tetrahydro-2H-phthalazin-1-one (20).

Method F, from 1-(chloromethyl)-2,3-dimethoxybenzene (634 mg, 3.4 mmol). Yield 69%. ^1H NMR (CDCl_3) δ 7.56 (d, $J = 1.8$ Hz, 1H), 7.28 (dd, $J = 1.8$, 8.4 Hz, 1H), 7.05–7.11 (m, 2H), 6.89 (d, $J = 8.5$ Hz, 2H), 5.74–5.81 (m, 1H), 5.62–5.70 (m, 1H), 5.27 (s, 2H), 4.76–4.83 (m, 1H), 3.92 (s, 3H), 3.89 (s, 3H), 3.87 (s, 3H), 3.23–3.29 (m, 1H), 2.95–3.05 (m, 1H), 2.70 (t, $J = 5.7$ Hz), 1.82–2.23 (m, 5H), 1.69–1.81 (m, 4H), 1.47–1.65 (m, 6H). LC–MS–ESI $^+$ m/z 519 [M+H] $^+$; HRMS–ESI $^+$ [M+H] $^+$ calcd for $\text{C}_{31}\text{H}_{39}\text{N}_2\text{O}_5$ 519.2853, found 519.2842.

4.2.2.12. *cis*-2-Cycloheptyl-4-[3-(3,5-dimethoxybenzyloxy)-4-methoxy-phenyl]-4a,5,8,8a-tetrahydro-2H-phthalazin-1-one (21).

Method F, from 1-(chloromethyl)-3,5-dimethoxybenzene (634 mg, 3.4 mmol). Yield: 59%. ^1H NMR (CDCl_3) δ 7.48 (d, $J = 1.9$ Hz, 1H), 7.29 (dd, $J = 1.9$, 8.5 Hz, 1H), 6.90 (d, $J = 8.5$ Hz, 1H), 6.62 (d, $J = 2.2$ Hz, 2H), 6.39 (t, $J = 2.2$ Hz, 1H), 5.73–5.81 (m, 1H), 5.61–5.69 (m, 1H), 5.17 (d, $J = 12.9$ Hz, 2H), 4.73–4.85 (m, 1H), 3.93 (s, 3H), 3.78 (s, 6H), 3.15–3.25 (m, 1H), 2.93–3.03 (m, 1H), 2.69 (t, $J = 5.8$ Hz, 1H), 1.81–2.23 (m, 5H), 1.66–1.81 (m, 4H), 1.42–1.66 (m, 6H). LCMS found 519.2 [M+H] $^+$. HRMS–ESI $^+$ [M+H] $^+$ calcd for $\text{C}_{31}\text{H}_{39}\text{N}_2\text{O}_5$ 519.2853, found 519.2844.

4.2.2.13. *cis*-2-Cycloheptyl-4-[4-methoxy-3-(pyridin-2-ylmethoxy)-phenyl]-4a,5,8,8a-tetrahydro-2H-phthalazin-1-one (22).

Method F, from 2-(chloromethyl)pyridine-HCl (558 mg, 3.4 mmol); in this case 4 equiv of potassium carbonate were added and the reaction mixture was stirred for 6 h at 65 °C; Yield: 47%. ^1H NMR (CDCl_3) δ 8.61 (d, $J = 4.0$ Hz, 1H), 7.72 (t, $J = 7.6$ Hz, 1H), 7.57 (d, $J = 7.8$ Hz, 1H), 7.48 (d, $J = 1.8$ Hz, 1H), 7.31 (dd, $J = 8.4$, 1.8 Hz,

1H), 7.20–7.25 (m, 1H), 6.92 (d, $J = 8.5$ Hz, 1H), 5.73–5.81 (m, 1H), 5.61–5.69 (m, 1H), 5.36 (s, 2H), 4.71–4.82 (m, 1H), 3.96 (s, 3H), 3.17–3.26 (m, 1H), 2.92–3.03 (m, 1H), 2.68 (t, $J = 5.8$ Hz, 1H), 1.80–2.23 (m, 5H), 1.40–1.80 (m, 10H). LC–MS–ESI $^+$ m/z 460 [M+H] $^+$; HRMS–ESI $^+$ [M+H] $^+$ calcd for $\text{C}_{28}\text{H}_{34}\text{N}_3\text{O}_3$ 460.2595, found 460.2607.

4.2.2.14. *cis*-2-Cycloheptyl-4-[4-methoxy-3-(pyridin-4-ylmethoxy)-phenyl]-4a,5,8,8a-tetrahydro-2H-phthalazin-1-one (23).

Method F, from 4-(chloromethyl)pyridine-HCl (558 mg, 3.4 mmol); in this case 4 equiv of potassium carbonate were added and the reaction mixture was stirred for 24 h at 65 °C. Then 1 equiv of potassium carbonate was added and the reaction mixture was stirred for additional 26 h at 90 °C; Yield: 37%. ^1H NMR (CDCl_3) δ 8.62 (d, $J = 5.6$ Hz, 2H), 7.45 (d, $J = 1.8$ Hz, 1H), 7.39 (d, $J = 5.6$ Hz, 2H), 7.28 (dd, $J = 8.4$, 1.8 Hz, 1H), 6.92 (d, $J = 8.4$ Hz, 1H), 5.74–5.81 (m, 1H), 5.61–5.70 (m, 1H), 5.25 (s, 2H), 4.73–4.83 (m, 1H), 3.96 (s, 3H), 3.19–3.38 (m, 1H), 2.94–3.04 (m, 1H), 2.68 (t, $J = 5.9$ Hz, 1H), 1.81–2.25 (m, 5H), 1.42–1.80 (m, 10H). LC–MS–ESI $^+$ m/z 460 [M+H] $^+$; HRMS–ESI $^+$ [M+H] $^+$ calcd for $\text{C}_{28}\text{H}_{34}\text{N}_3\text{O}_3$ 460.2595, found 460.2597.

4.2.2.15. *cis*-2-Cycloheptyl-4-[3-[2-(4-dimethylaminophenyl)-ethoxy]-4-methoxy-phenyl]-4a,5,8,8a-tetrahydro-2H-phthalazin-1-one (24).

Method G, from 2-(4-dimethylaminophenyl) ethanol (45 mg, 0.27 mmol); Yield: 25%. ^1H NMR (CDCl_3) δ 7.50 (d, $J = 1.8$ Hz, 1H), 7.30 (dd, $J = 8.5$, 1.8 Hz, 1H), 7.19 (d, $J = 8.6$ Hz, 2H), 6.89 (d, $J = 8.5$ Hz, 1H), 6.72 (d, $J = 8.6$ Hz, 2H), 5.74–5.82 (m, 1H), 5.63–5.70 (m, 1H), 4.77–4.87 (m, 1H), 4.24 (t, $J = 8.0$ Hz, 2H), 3.92 (s, 3H), 3.24–3.31 (m, 1H), 3.10 (t, $J = 7.9$ Hz, 2H), 2.94–3.05 (m, 1H), 2.93 (s, 6H), 2.71 (t, $J = 5.7$ Hz, 1H), 1.81–2.25 (m, 5H), 1.42–1.80 (m, 10H). LC–MS–ESI $^+$ m/z 516 [M+H] $^+$; HRMS–ESI $^+$ [M+H] $^+$ calcd for $\text{C}_{32}\text{H}_{42}\text{N}_3\text{O}_3$ 516.3221, found 516.3228.

4.2.2.16. *cis*-2-Cycloheptyl-4-[3-[2-(4-methoxyphenyl)-ethoxy]-4-methoxy-phenyl]-4a,5,8,8a-tetrahydro-2H-phthalazin-1-one (25).

Method G, from 2-(4-methoxyphenyl) ethanol (41 mg, 0.27 mmol); Yield: 23%. ^1H NMR (CDCl_3) δ 7.50 (d, $J = 1.8$ Hz, 1H), 7.29 (dd, $J = 8.0$, 1.9 Hz, 1H), 7.23 (d, $J = 8.5$ Hz, 2H), 6.83–6.93 (m, 3H), 5.73–5.83 (m, 1H), 5.63–5.71 (m, 1H), 4.76–4.87 (m, 1H), 4.26 (t, $J = 7.6$ Hz, 2H), 3.92 (s, 3H), 3.80 (s, 3H), 3.23–3.31 (m, 1H), 3.13 (t, $J = 7.6$ Hz, 2H), 2.96–3.06 (m, 1H), 2.71 (t, $J = 5.8$ Hz, 1H), 1.86–2.25 (m, 5H), 1.44–1.86 (m, 10H). LC–MS–ESI $^+$ m/z 503 [M+H] $^+$; HRMS–ESI $^+$ [M+H] $^+$ calcd for $\text{C}_{31}\text{H}_{39}\text{N}_2\text{O}_4$ 503.2904, found 503.2915.

4.3. Determination of PDE activity

The standard scintillation proximity assay (SPA) for determination of PDE activities was used to analyze effects of test compounds on the enzymatic activities of TbrPDEB1 and TbrPDEB2¹ and full length human recombinant PDE1B1, 2A3, 3A1, 4B1, 4B2, 4D3, 5A1, 7A1, 8B, 10A and 11A4.³¹ In these assays, the cAMP or cGMP (PDE5A1) substrate concentration was 0.5 μM .

4.4. In vitro susceptibility testing of trypanosomes and MRC-5 fibroblasts

T. b. brucei (Squib-427 strain, suramin-sensitive) trypomastigotes or MRC-5 fibroblasts were cultured at 37 °C and 5% CO_2 in Hirumi-9 medium, supplemented with 10% fetal calf serum (FCS) as described previously.²³ Compound stock solutions were prepared in 100% DMSO at 20 mM. The compounds were serially pre-diluted (2-fold or 4-fold) in DMSO followed by a further (intermediate) dilution in demineralized water to assure a final in-test DMSO concentration of <1%.

Author contributions

The manuscript was written through contributions of all authors. All authors have given approval to the final version of the manuscript. All authors contributed equally.

Acknowledgements

This research was performed under the framework of the Top Institute Pharma project 'Phosphodiesterase inhibitors for Neglected Tropical Diseases' with partners the VU University Amsterdam, University of Bern, The Royal Tropical Institute, Netherlands, Mercachem BV, Nycomed: a Takeda Company, IOTA Pharmaceuticals Ltd, the Drugs for Neglected Diseases initiative (DNDi) and TI Pharma. DNDi is grateful to its donors, public and private, who have provided funding to DNDi since its inception in 2003. With the support of these donors, DNDi is well on its way to achieving the objectives of building a robust pipeline and delivering 11–13 new treatments by 2018. A full list of DNDi's donors can be found at <http://www.dndi.org/donors/donors.html>. For the work described in this paper, DNDi allocated non-earmarked funding from the following donors: The Bill & Melinda Gates Foundation (BMGF)/United States of America, Reconstruction Credit Institution-Federal Ministry of Education and Research (KfW-BMBF)/Germany and Médecins Sans Frontières (Doctors without Borders)/International. The donors had no role in study design, data collection and analysis, decision to publish, or preparation of the manuscript.

References and notes

- De Koning, H. P.; Gould, M. K.; Sterk, G. J.; Tenor, H.; Kunz, S.; Luginbuehl, E.; Seebeck, T. *J. Infect. Dis.* **2012**, *206*, 229.
- Simarro, P. P.; Diarra, A.; Postigo, J. A. R.; Franco, J. R.; Jannin, J. G. *PLoS Neglected Trop. Dis.* **2011**, *5*, e1007.
- Fèvre, E. M.; Wissmann, B. V.; Welburn, S. C.; Lutumba, P. *PLoS Neglected Trop. Dis.* **2008**, *2*, e333.
- Kennedy, P. G. *Ann. Neurol.* **2008**, *64*, 116.
- Oberholzer, M.; Marti, G.; Baresic, M.; Kunz, S.; Hemphill, A.; Seebeck, T. *FASEB J.* **2007**, *21*, 720.
- Conti, M.; Beavo, M. *Annu. Rev. Biochem.* **2007**, *76*, 481.
- Seebeck, T.; Sterk, G. J.; Ke, H. *Future Med. Chem.* **2011**, *3*, 1289.
- Shakur, Y.; de Koning, H. P.; Ke, H.; Kambayashi, J.; Seebeck, T. Therapeutic Potential of Phosphodiesterase Inhibitors in Parasitic Diseases. In *Handb. Exp. Pharmacol.*; Francis, S. H., Conti, M., Houslay, M. D., Eds.; Springer: Berlin and Heidelberg, Germany, 2011; pp 487–510.
- Pollastri, M. P.; Campbell, R. K. *Future Med. Chem.* **2011**, *3*, 1307.
- Orrling, K. M.; Jansen, C.; Vu, X. L.; Balmer, V.; Bregy, P.; Shanmugham, A.; England, P.; Bailey, D.; Cos, P.; Maes, L.; Adams, E.; Van den Bogaart, E.; Chatelain, E.; Ioset, J.-P.; Van de Stolpe, A.; Zorg, S.; Veerman, J.; Seebeck, T.; Sterk, G. J.; De Esch, I. J. P.; Leurs, R. J. *Med. Chem.* **2012**, *55*, 8745.
- Bland, N. D.; Wang, C. H.; Tallman, C.; Gustafson, A. E.; Wang, Z.; Ashton, T. D.; Ochiana, S. O.; McAllister, G.; Cotter, K.; Fang, A. P.; Gechijian, L.; Garceau, N.; Gangurde, R.; Ortenberg, R.; Ondrechen, M. J.; Campbell, R. K.; Pollastri, M. P. *J. Med. Chem.* **2011**, *54*, 8188.
- Zoraghi, R.; Seebeck, T. *Proc. Natl. Acad. Sci. U.S.A.* **2002**, *99*, 4343.
- Wang, C.; Ashton, T. D.; Gustafson, A.; Bland, N. D.; Ochiana, S. O.; Campbell, R. K.; Pollastri, M. P. *Bioorg. Med. Chem. Lett.* **2012**, *22*, 2579.
- Ochiana, S. O.; Gustafson, A.; Bland, N. D.; Wang, C.; Russo, M. J.; Campbell, R. K.; Pollastri, M. P. *Bioorg. Med. Chem. Lett.* **2012**, *22*, 2582.
- Woodring, J. L.; Bland, N. D.; Ochiana, S. O.; Campbell, R. K.; Pollastri, M. P. *Bioorg. Med. Chem. Lett.* **2013**, *23*, 5971.
- Amata, E.; Bland, N. D.; Hoyt, C. T.; Settimo, L.; Campbell, R. K.; Pollastri, M. P. *Bioorg. Med. Chem. Lett.* **2014**, *24*, 4084.
- Amata, E.; Bland, N. D.; Campbell, R. K.; Pollastri, M. P. *Tetrahedron Lett.* **2015**, *2832*.
- Van der Mey, M.; Hatzelmann, A.; Van Klink, G. P.; Van der Laan, I. J.; Sterk, G. J.; Thibaut, U.; Ulrich, W. R.; Timmerman, H. *J. Med. Chem.* **2001**, *44*, 2523.
- Souness, J. E.; Aldous, D.; Sargent, C. *Immunopharmacology* **2000**, *47*, 127.
- Raychaudhuri, S. P.; Nguyen, C. T.; Raychaudhuri, S. K.; Gershwin, M. E. *Autoimmun. Rev.* **2009**, *9*, 67.
- Seldo, P. M.; Barnes, P. J.; Mejia, K.; Giembycs, M. A. *Mol. Pharmacol.* **1995**, *48*, 747.
- Van der Mey, M.; Boss, H.; Hatzelmann, A.; Van der Laan, I. J.; Sterk, G. J.; Timmerman, H. *J. Med. Chem.* **2002**, *45*, 2520.
- Takii, T.; Yamamoto, Y.; Chiba, T.; Abe, C.; Belisle, J. T.; Brennan, P. J.; Onozaki, K. *Antimicrob. Agents Chemother.* **2002**, *46*, 2533.
- Räz, B.; Iten, M.; Grether-Bühler, Y.; Kaminsky, R.; Brun, R. *Acta Trop.* **1997**, *68*, 139.
- Wang, H.; Yan, Z.; Geng, J.; Kunz, S.; Seebeck, T.; Ke, H. *Mol. Microbiol.* **2007**, *66*, 1029.
- Jansen, C.; Wang, H.; Kooistra, A. J.; De Graaf, C.; Orrling, K. M.; Tenor, H.; Seebeck, T.; Bailey, D.; De Esch, I. J. P.; Ke, H.; Leurs, R. J. *Med. Chem.* **2013**, *56*, 2087.
- Molecular Operating Environment, version 2010.10*; Chemical Computing Group (CCG): Montreal, Canada, 2010.
- Korb, O.; Stützle, T.; Exner, T. E. *J. Chem. Inf. Model.* **2009**, *49*, 84.
- Van der Mey, M.; Boss, H.; Hatzelmann, A.; Van der Laan, I. J.; Sterk, Thibaut U.; Timmerman, H. *J. Med. Chem.* **2001**, *44*, 2511.
- Van der Mey, M.; Bommelé, K. M.; Boss, H.; Hatzelmann, A.; Van Slingerland, M.; Sterk, G. J.; Timmerman, H. *J. Med. Chem.* **2003**, *46*, 2008.
- Hatzelmann, A.; Morcillo, E. J.; Lungarella, G.; Adnot, S.; Sanjar, S.; Beume, R.; Schudt, C.; Tenor, H. *Pulm. Pharmacol. Ther.* **2010**, *23*, 235.